DNA AND CELL BIOLOGY
Volume 00, Number 00, 2011

Pp. 1–9
DOI: 10.1089/dna.2010.1149

ORIGINAL RESEARCH ARTICLE

# A Novel Interaction Between Interferon-Inducible Protein p56 and Ribosomal Protein L15 in Gastric Cancer Cells

Yu-An Hsu,[1,*] Hui-Ju Lin,[2,*] Jim J.C. Sheu,[3,4] Fa-Kuen Shieh,[5] Shih-Yin Chen,[3,4] Chih-Ho Lai,[6] Fuu-Jen Tsai,[3,7] Lei Wan,[3,4,8] and Bing-Hung Chen[9]

Type I interferons (IFNs) are potent inducers of antiviral and antiproliferative activities in vertebrates. IFNs cause activation of genes encoding antiviral proteins, such as p56 from the IFN-stimulated gene family. There are six tetratricopeptide repeat (TPR) motifs located at the N-terminal sequence of p56. Since TPR motifs are known to participate in protein-protein interactions, p56 may associate with various large protein complexes to modify their functions. Using a T7 phage display library, we identified ribosomal protein L15 (RPL15) as a novel interacting partner of p56. The p56-RPL15 interaction was confirmed by pull-down assays. Overexpression of p56 exhibited strong inhibition on the growth of RPL15-overexpressing cancer cells. Small interfering RNA targeting RPL15 not only reduced the growth rate of gastric cancer cells but also sensitized these cells to type I IFN-induced proliferative inhibition. Using site-directed mutagenesis, we also mapped the TPRs 1–4 of p56 as crucial domains to interact with RPL15. Taken together, our results demonstrated a novel interaction between p56 and RPL15. Differential regulation of p56 and RPL15 expression contributes to the antiproliferative capacity on gastric cancer cells, and further elucidation of their interaction may facilitate the development of new anticancer regimens.

## Introduction

Type I interferons (IFNs) promote both antiviral and antiproliferative activities in vertebrates. Recombinant IFNα is approved for treating more than 14 malignancies and several viral diseases in over 40 countries (Pfeffer *et al.*, 1998; Caraglia *et al.*, 2005, 2009). IFNα is often used in combination with chemotherapy for the treatment of metastatic melanoma, condyloma acuminata, Kaposi's sarcoma, and hepatitis B and C (Parmar and Platanias, 2003; Caraglia *et al.*, 2005; Wan *et al.*, 2009). IFNs have pleiotropic effects on many aspects of cell physiology and are considered an indispensable component of the innate immune response (Sadler and Williams, 2008). Among various IFN-inducible proteins, p56 is a tetratricopeptide repeat (TPR)-containing protein and belongs to a viral stress-inducible protein family whose members also include p54, p58, and p60 (Guo *et al.*, 2000; Sarkar and Sen, 2004; Terenzi *et al.*, 2005; Terenzi *et al.*, 2006). The molecular and biochemical properties of these proteins have not been fully characterized. p56 expression, undetectable when inducers were absent (Guo *et al.*, 2000; Terenzi *et al.*, 2005), can be highly induced by IFN, double-stranded RNA, and viral infections, albeit such induction was often transient with rapid turn-over rates at both mRNA and protein levels (Guo *et al.*, 2000; Sarkar and Sen, 2004). Human p56 inhibits protein synthesis by interacting with the eukaryotic initiation factor 3e (eIF3e) subunit of eIF3 complex to prevent formation of the eIF2 · GTP · Met-tRNAi ternary complex during translation (Hui *et al.*, 2003). However, mouse p56 inhibits translation by a different mechanism; it binds to eIF3c and prevents its association with the 20S and 40S ribosomal subunits (Hui *et al.*, 2005). The eIF3-p56 interaction is mediated by cooperation among the proteasome, COP9-signalosome and initiation factor (PCI) complex, and TPR motifs, with both TPRs 5 and 6 of p56 being required for the interaction to occur (Guo and Sen, 2000; Sarkar and Sen, 2004). Moreover, p56 inhibits DNA replication of human papillomaviruses (HPV) by interacting with the C-terminal

[1]Department of Life Science, National Tsing Hua University, Hsinchu, Taiwan.
[2]Department of Ophthalmology and [3]Genetic Center, China Medical University Hospital, Taichung, Taiwan.
[4]School of Chinese Medicine, China Medical University, Taichung, Taiwan.
[5]Department of Chemistry, National Central University, Taoyuan, Taiwan.
[6]Department of Microbiology, School of Medicine, China Medical University, Taichung, Taiwan.
[7]School of Post-Baccalaureate Chinese Medicine, China Medical University, Taichung, Taiwan.
[8]Department of Biotechnology, Asia University, Taichung, Taiwan.
[9]Department of Biotechnology, Kaohsiung Medical University, Kaohsiung, Taiwan.
*These authors contributed equally to this work.

region of the DNA replication origin-binding protein E1 of HPV via its N-terminal TPR 2 motif (Terenzi *et al.*, 2008).

Structurally, the TPR motif is a degenerate sequence of 34 amino acids, occurring in tandem arrays of 3–16 motifs, that mediates protein-protein interactions and the formation of multiprotein complexes (Sikorski *et al.*, 1990; Blatch and Lassle, 1999). Although various TPR motifs reveal a large degree of sequence diversity, structural comparison shows a highly conserved three-dimensional structure of TPRs from proteins possessing this motif (Blatch and Lassle, 1999). A typical TPR domain is composed of a helix-turn-helix arrangement (Goebl and Yanagida, 1991; Blatch and Lassle, 1999). p56 may associate with various large protein complexes, via its TPR motifs, to modify their functions. In the current study, we identified the ribosomal protein L15 (RPL15) as a novel p56-interacting partner from a human splenic T7 page display library. We also provided evidence that either over-expressing p56 or down-regulating RPL15 exhibited antiproliferative potential on human gastric cancer cells. Additionally, we mapped the TPRs 1–4 of p56 as the motifs crucial for its interaction with RPL15. This novel observation may provide insights into the design of potential anticancer regimens for gastric cancers.

## Materials and Methods

### *Reagents and cells*

Dulbecco's modified Eagle's medium, Dulbecco's phosphate-buffered saline (PBS), L-glutamine, and ampicillin were obtained from Invitrogen (Carlsbad, CA). Fetal bovine serum was purchased from Hyclone (Logan, UT). Protein assay reagents were obtained from Bio-Rad Laboratories (Richmond, CA). FugeneHD transfection reagent was purchased from Roche Applied Science (Indianapolis, IN). Antibodies (Abs) against various tags [glutathione-S-transferase (GST), polyhistidine (His), c-Myc, and FLAG] were from Sigma-Aldrich (St. Louis, MO). Anti-IFIT1, anti-RPL15 Abs, and recombinant RPL15-GST were from Abnova (Taipei, Taiwan). Anti-GST, anti-His, anti-c-Myc, and anti-FLAG M1 agarose slurries were from Sigma-Aldrich. Protease inhibitor cocktail and 3-(4,5-dimethylthiazol-2-yl)-2,5-diphenyltetrazolium bromide (MTT) were from Sigma-Aldrich. The Imperial Protein Stain Kit was obtained from Thermo Scientific (Rockford, IL). The T7Select10-3b vector (Novagen, Madison, WI) was used for the construction of human splenic cDNA display library.

Human gastric adenocarcinoma cell lines, MKN45 (JCRB0254; JCRB, Osaka, Japan) and AGS (BCRC60102; BCRC, Hsin-Chu, Taiwan), were maintained as adherent cultures in Dulbecco's modified Eagle's medium supplemented with 10% fetal bovine serum. The cells were incubated at 37°C in a humidified atmosphere with 5% $CO_2$.

### *Oligonucleotides for plasmid construction*

Oligonucleotides designed for this study are as follows (with the corresponding plasmid and tag sequence shown in preceding parenthesis): (pET21a, His) p56-His, 5′-AAAGCT AGCATGAGTACAAATGGTGATGA-3′ (f), 5′-AAACTCGA GAGGACCTTGTCTCACAGAGT-3′ (r); (pcDNA3, FLAG) p56-FLAG, 5′-AAAGGATCCATGAGTACAAATGGTGAT GA-3′ (f), 5′-TTTCTCGAGTTACTACTTATCGTCGTCATCC TTGTAATCAAATGTGGGCTTTTTTTC-3′ (r); (pTriEX4, FLAG) TPRΔ1-2, 5′-AAAGGATCCATGTCAAATCCCTTCC GCTAT-3′ (f), 5′-TTTCTCGAGTTACTACTTATCGTCGT CATCCTTGTAATCAGGACCTTGTCTCACAGAGTT-3′ (r); (pTriEX4, FLAG) TPRΔ3-4_p1-182, 5′-AAAGGATCCAT GAGTACAAATGGTGATGAT-3′ (f), 5′-TGATGCAGTAA GACCGCATACCCA-3′ (r); (pTriEX4, FLAG) TPRΔ3-4_p295-478, 5′-TATGCGGTCTTACTGCATCACCAGAT-3′ (f), 5′-TTTCTCGAGTTACTACTTATCGTCGTCATCCTTG TAATCAGGACCTTGTCTCACAGAGTT-3′ (r); (pTriEX4, FLAG) TPRΔ5-6, 5′-AAAGGATCCATGAGTACAAATGG TGATGAT-3′ (f), 5′-TTTCTCGAGTTACTACTTATCGTCGT CATCCTTGTAATCAAATGTGGGCTTTTTTTC-3′ (r); (pTriEX4, c-Myc) RPL15-Myc, 5′-AAACCATGGGGATGGGTGCATAC AAGTACAT-3′ (f), 5′-TTTCTCGAGCTACAGATCCTCTTC TGAGATGAGTTTTTGTTCGCGGTAACGGTGGAGC-3′ (r).

### *Preparation of recombinant p56*

Complementary DNA (cDNA) sequence of p56 was amplified with the p56-His primers and ligated into pET21a plasmid. Induction of recombinant p56-His was performed with the addition of 0.5 mM isopropyl β-d-thiogalactoside (IPTG) to transformed *Escherichia coli* BL21(DE3) strain. The cells were harvested 4 h postinduction by centrifugation, and the pellets were dissolved in buffer A (6 M guanidine hydrochloride, 300 mM NaCl, 20 mM Tri-HCl, pH 8.0) followed by sonication four times for 30 s each time. The insoluble debris was removed by centrifugation after sonication, and the clarified supernatant was then mixed with TALON metal-affinity resins that had been previously immersed and equilibrated with buffer A. The mixture was gently agitated at room temperature for 1 h and centrifuged at 500*g* for 10 min. The supernatant was discarded, and the resins were washed three times with buffer A. The washed resins were resuspended in buffer A and packed into a purification column (0.5×4 cm). In-column renaturation of p56-His was achieved by applying a slow concentration gradient from buffer A to buffer B (same as buffer A, except no guanidine hydrochloride) onto the column. Finally, the p56-His proteins were eluted with buffer C (buffer A containing 400 mM imidazole) and dialyzed into PBS for use in the experiments.

### *Polymerase chain reaction*

Total RNA was isolated from untreated or treated cells using RNeasy Mini Kit (Qiagen, Hilden, Germany). Real-time quantative PCR (qPCR) was performed on a LightCycler480 (Roche Applied Science, Mannheim, Germany) using the High-Capacity cDNA Reverse Transcription Kit system (Applied Biosystems, Foster City, CA) and the Universal Probe (Roche Applied Science) according to the manufacturer's instructions. The probes used and their sequences were as follows: Glyceraldehyde-3-phosphate dehydrogenase (GAPDH): 5′-AGCCACATCGCTCAGACA-3′ (f), 5′-GCCCAATACGACCAAATCC-3′ (r); p56: 5′-AGAA CGGCTGCCTAATTTACAG-3′ (f), 5′-GCTCCAGACTAT CCTTGACCTG-3′ (r); RPL15: 5′-CCAGCTAAAGTTTGC TCGAAG-3′ (f), 5′-GACTCTCAGAGCCCCACAGT-3′ (r). Reverse-transcription PCR (RT-PCR) was performed at 37°C for 2 h, and the cycling parameters were as follows: denaturation at 95°C for 10 min, amplification at 95°C for 10 s and 60°C for 15 s, for a total of 45 cycles. Each reaction was carried out in

triplicate. For normalization, transcripts of *GAPDH* were quantified as endogenous RNA reference to normalize each sample. The results were normalized as relative expression that the average value of the test sample mRNA was divided by the average value of *GAPDH* mRNA. The ratio was calculated by dividing the normalized values of cells in the experimental groups by the value in untreated control cells.

### *Cell proliferation assay*

Cell proliferation was determined by MTT assay. Briefly, cells were seeded on a 96-well plate at $1\times10^3$ cells/well and allowed to attach for 24 h. After transfection or treatment with IFNs, the medium was carefully removed and replaced with 90 μL of fresh culture medium. Cells were added with MTT solution (0.5 mg/mL) at 10 μL/well and incubated for an additional 4 h to allow the conversion of MTT into formazan. At the end of incubation, the medium was removed, and the precipitates were solubilized by adding 200 μL of DMSO/ethanol (1:1, v/v) solution. The amount of formazan formed, indicative of the cell's proliferative capacity, was determined by measuring the absorbance at 570 nm using an ELISA plate reader (Molecular Devices, Sunnyvale, CA).

### *Western blotting*

Proteins or cell extracts were subjected to sodium dodecyl sulphate–polyacrylamide gel electrophoresis using a 12% separation gel and blotted onto a polyvinylidene difluoride membrane (Millipore, Billerica, MA). The membrane was incubated with 4% skim milk solution for 1 h at 25°C, followed by incubation with primary Abs overnight at 4°C. The membrane was then washed and probed with a species-specific antibody conjugated with horseradish peroxidase (HRP). For visualization, binding of proteins was detected by SuperSignal West Pico Chemiluminescent Substrate (Pierce, Rockford, IL) according to the manufacturer's instructions. Blots shown are representative of at least three individual experiments.

### *Coimmunoprecipitation assay*

Coimmunoprecipitation was performed on MKN45 cells that had been cotransfected with the pTriEX4-RPL15-Myc plasmid and another pTriEX4 plasmid carrying either full-length p56 or p56 with variable truncated TPR domains (denoted as TPRΔ1-2, TPRΔ3-4, and TPRΔ5-6). After transfection, MKN45 cells were cultured at 37°C in 5% $CO_2$ for 24 h. Cells were washed with 10 mL of PBS three times and lysed with M-PER (Pierce, Rockford, IL) containing a protease inhibitor cocktail. After removing the insoluble debris by centrifugation, the lysates were incubated with anti-FLAG M1 or anti-c-Myc agarose (Sigma-Aldrich). The antibody-protein complexes were collected by centrifugation, washed, eluted by boiling in protein sample buffer, separated by sodium dodecyl sulphate–polyacrylamide gel electrophoresis, and western blotted using HRP-conjugated anti-FLAG Ab as described above.

### *Statistical analysis*

All values are means ± SD of three independent experiments. Data were analyzed by Student's *t*-test or one-way ANOVA. Statistical significance was determined with $p < 0.05$.

## Results

### *Identification of RPL15 as a p56-interacting protein*

Our protocol yielded a relatively high purity (>90% by commassie blue staining) (Fig. 1A, arrow) recombinant human p56-His protein from BL21 *E. coli*. Using this p56-His as the bait to screen a human splenic cDNA T7 phage display library, a total of 1,000 positive cells were selected by biopanning and sequenced. All cDNA sequences were translated into peptide sequences and searched against the NCBI database for putative p56-interacting peptides. The peptide sequence from clone 16–43 was found to completely match the C-terminal 87 residues of human RPL15 (GenBank ID: AAH14837.1).

To determine the interaction between p56 and RPL15, a pull-down assay was performed with p56-His and RPL15-GST proteins. Our result showed that recombinant p56 and RPL15 proteins bound to each other and they could be pulled down together with either anti-His (Fig. 1B, lane 2) or anti-GST agarose (Fig. 1C, lane 4). Appropriate controls were performed to demonstrate that binding of p56-His or RPL15-GST to their respective agarose slurries was specific (Fig. 1B, C, lanes 1 and 3). To further confirm that p56-His is being pulled down by RPL15-GST and not the GST alone, a control experiment was performed by incubating p56-His and GST before the addition of either anti-His or anti-GST agarose. p56-His was specifically bound by the anti-His agarose (Fig. 1D, arrow) and exhibited no nonspecific interaction with GST (Fig. 1D, arrow head). Therefore, our results demonstrated that a novel and stable interaction occurred between p56 and RPL15.

### *Overexpression of p56 or downregulation of RPL15 inhibits the proliferation of gastric cancer cells*

RPL15 is markedly increased in human gastric cancer cells. To understand the roles of both RPL15 and p56 on the proliferative ability of gastric cancers, AGS and MKN45 cells were separately transfected with either RPL15 small interfering RNA (siRNA) (siRPL15) or plasmid carrying p56. Since p56 is the protein product of mRNA 561 encoded by the *IFIT1* gene, we first sought to determine the mRNA levels of both *RPL15* and *IFIT1* genes in both cell lines. Real-time qPCR experiments were performed using RNA harvested from either untransfected or day 4 post-transfection cells. When compared with untransfected controls, the *RPL15* mRNA levels exhibited a 60% and 55% reduction in AGS and MNK45 cells, respectively, after the siRNA treatment (Fig. 2A). On the other hand, both p56-transfected cell lines exhibited a significant increase in *IFIT1* mRNA levels (about 14- and 9-fold increase, respectively) in comparison with the untransfected controls (Fig. 2B).

Proliferation of siRPL15- and p56-transfected cells was monitored for 5 days after transfection. Starting 72 h post-transfection, a significant inhibition on proliferation was observed in both siRPL15-transfected cell lines (Fig. 2C, open symbols), indicative of the role that RPL15 plays in promoting cell growth. On the other hand, overexpression of p56 caused a significant proliferative inhibition (Fig. 2D, open symbols),

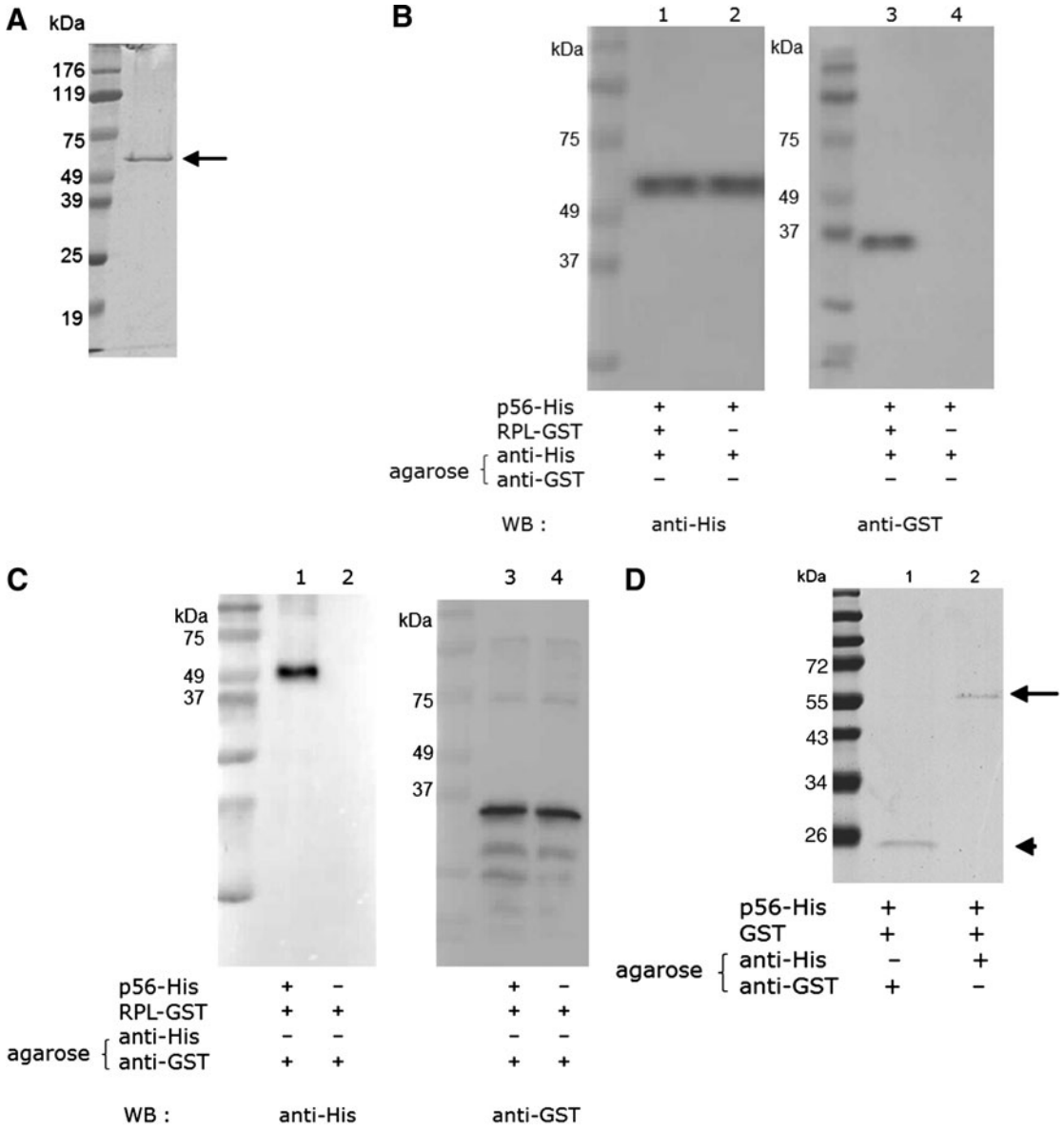


**FIG. 1.** Purification of recombinant p56 and identification of p56-ribosomal protein L15 (RPL15) interaction. **(A)** His-tagged recombinant p56 (arrow) was expressed and purified from BL21 *E. coli* and analyzed by sodium dodecyl sulphate–polyacrylamide gel electrophoresis (SDS-PAGE) with an apparent m.w. of 56 kDa. Equal amounts (5 μg each) of RPL15-GST and p56-His were mixed together **(**lanes 1 and 3, in both **B** and **C)**, or left alone **(**lanes 2 and 4, in both **B** and **C)**, followed by incubation at 4°C for overnight. Then, the mixtures were incubated with either anti-His **(B)** or anti-GST **(C)** agarose for 4 h. After washing and centrifugation, aliquots of agarose were boiled and subjected to SDS-PAGE and western blotting with anti-His or anti-GST Abs. **(D)** Recombinant p56-His and GST were mixed and incubated at 4°C for 4 h before equally divided to be incubated with either anti-His or anti-GST agarose. Bound proteins were analyzed by SDS-PAGE, and the presence of p56-His (arrow) and GST (arrow head) was indicated.

and such inhibition was observed as early as day 2 post-transfection. We also performed western blotting to compare the p56 levels in AGS and MKN45 cells transfected with plasmid carrying p56 construct. Cell lysates from AGS and MKN45 cells transfected with pcDNA3-FLAG-p56 plasmids showed significantly elevated levels of recombinant p56 (lanes 2 and 4, Fig. 2E) as detected by the anti-FLAG Ab, whereas transfectants with empty vector (lanes 1 and 3, Fig. 2E) only exhibited basal levels of the FLAG signals.

Additionally, we tested the effects of transfection using mock vectors (Fig. 2F, filled symbols) or vectors containing scrambled RNA (Fig. 2F, open symbols) in both AGS and MKN45 gastric cancer cells. The proliferation of AGS cells transfected with control scrambled RNA only exhibited marginal inhibition as compared with the same transfection control inMKN45 cells. However, there was still a significant inhibition on proliferation of both AGS and MKN45 cells transfected with the siRPL15 plasmids, demonstrating the negative effects of knocking-down RPL15 on proliferation of both cell lines. Similarly, transfection of AGS and MKN45 cells with mock pcDNA3-FLAG plasmid did not affect proliferation of the cells (Fig. 2G, filled symbols). However,

transfection with plasmid carrying a p56 construct significantly inhibited proliferation of both cell types (Fig. 2G, open symbols), suggesting an inhibitory effect of p56 on proliferation of AGS and MKN45 cells.

Therefore, our data suggested that the RPL15 and/or p56 levels could influence the proliferative potential of human gastric cancer cells.

### *Overexpression of p56 or downregulation of RPL15 increases the type I IFN-induced antiproliferation effects*

IFN treatments inhibit cell proliferation in various cancers (Hasan *et al.*, 2007; Katsoulidis *et al.*, 2009). Expression of p56 is undetectable when IFN is absent. When treated with IFN, p56 expression increases more than 1000-fold in both mRNA and protein levels. Therefore, under normal conditions, p56 is absent and will not inhibit the growth of the cells. We sought to determine whether the change of either RPL15 or p56 level would affect type I IFN-induced inhibition on cell proliferation in gastric cancer cells. AGS cells exhibited a 21%–31% and 13%–20% growth inhibition in a dose-dependent manner when treated with IFNα and IFNβ, respectively (Fig. 3A, gray bars). A more prominent growth inhibition (27%–54% and 25%–52% for IFNα and IFNβ, respectively) was observed when the same IFN treatments were applied to the AGS-siRPL15 cells whose endogenous RPL15 was knocked down (Fig. 3A, black

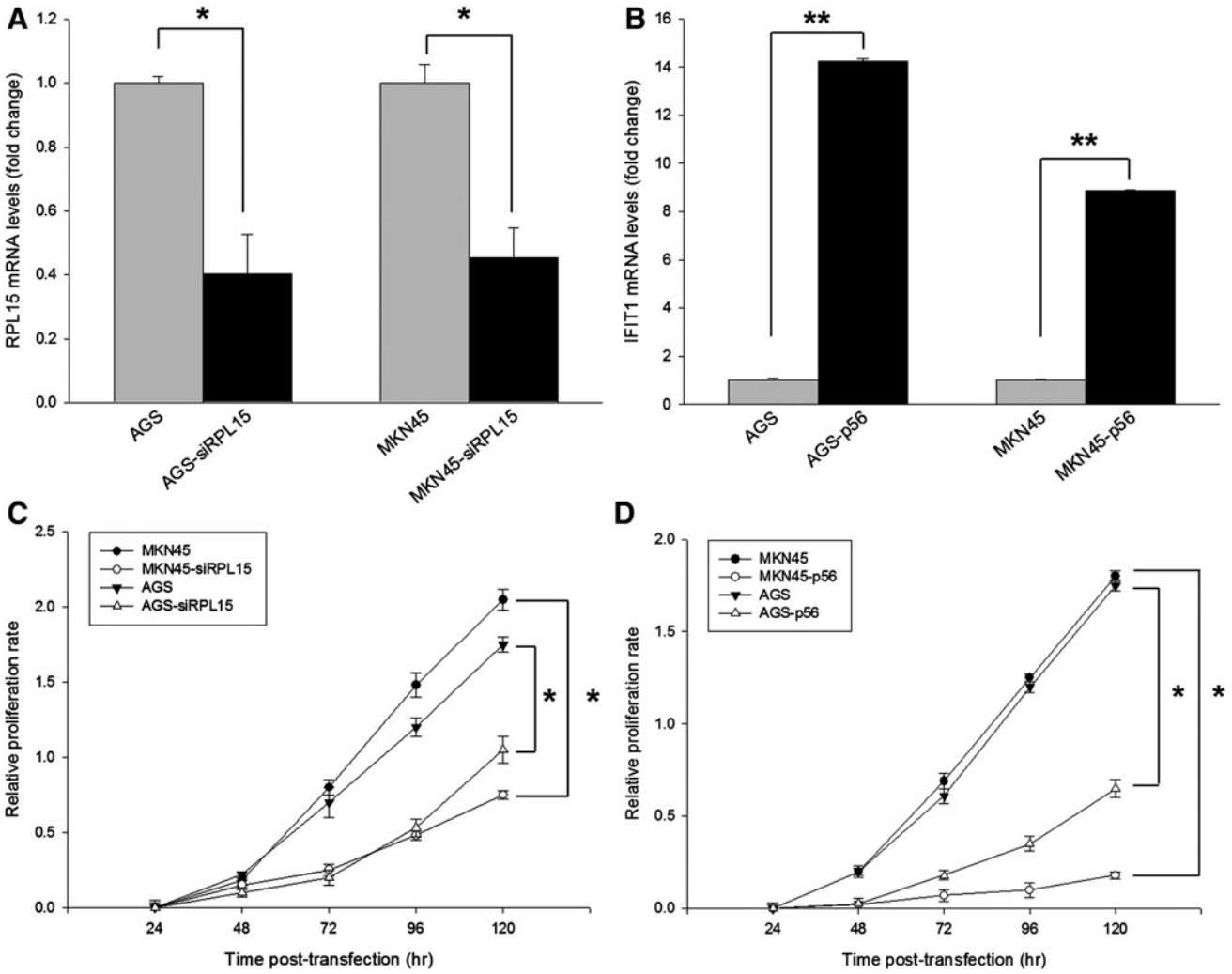


**FIG. 2.** Knock-down of RPL15 or overexpression of p56 contributed to growth inhibition on gastric cancer cells. Human gastric cancer cells, AGS and MKN45, were transfected with either RPL15-small interfering RNA (siRNA) or plasmid carrying p56 for 48 h. Total RNA was extracted and subjected to real-time qPCR on expression levels of **(A)** *RPL15* or **(B)** *IFIT1* mRNA. Levels of *GAPDH* transcripts were used as endogenous RNA of reference for the normalization of each sample. Cell proliferation was measured on untreated cells **(C** and **D,** closed symbols**)** or cells treated with RPL15 siRNA or p56-carrying plasmid **(C** and **D,** open symbols**)** on days 1–5 post-transfection by MTT assay. **(E)** Lysates from p56-FLAG-transfected AGS and MKN45 cells were subjected to western blotting analysis for the presence of recombinant p56 proteins (lanes 2 and 4). **(F, G)** Mock vectors (filled symbols) or vectors carrying either scramble RNA **(F,** open symbols**)** or p56-FLAG **(G,** open symbols**)** were used to test the transfection in both AGS and MKC45 cells. Proliferation of all transfectants was tested with MTT assay on days 1–5 post-transfection. Values are means ± SD of three independent experiments. Asterisk indicates statistical significance as determined by Student's *t*-test (*$p < 0.05$, **$p < 0.01$).

(*Figure continues*→)

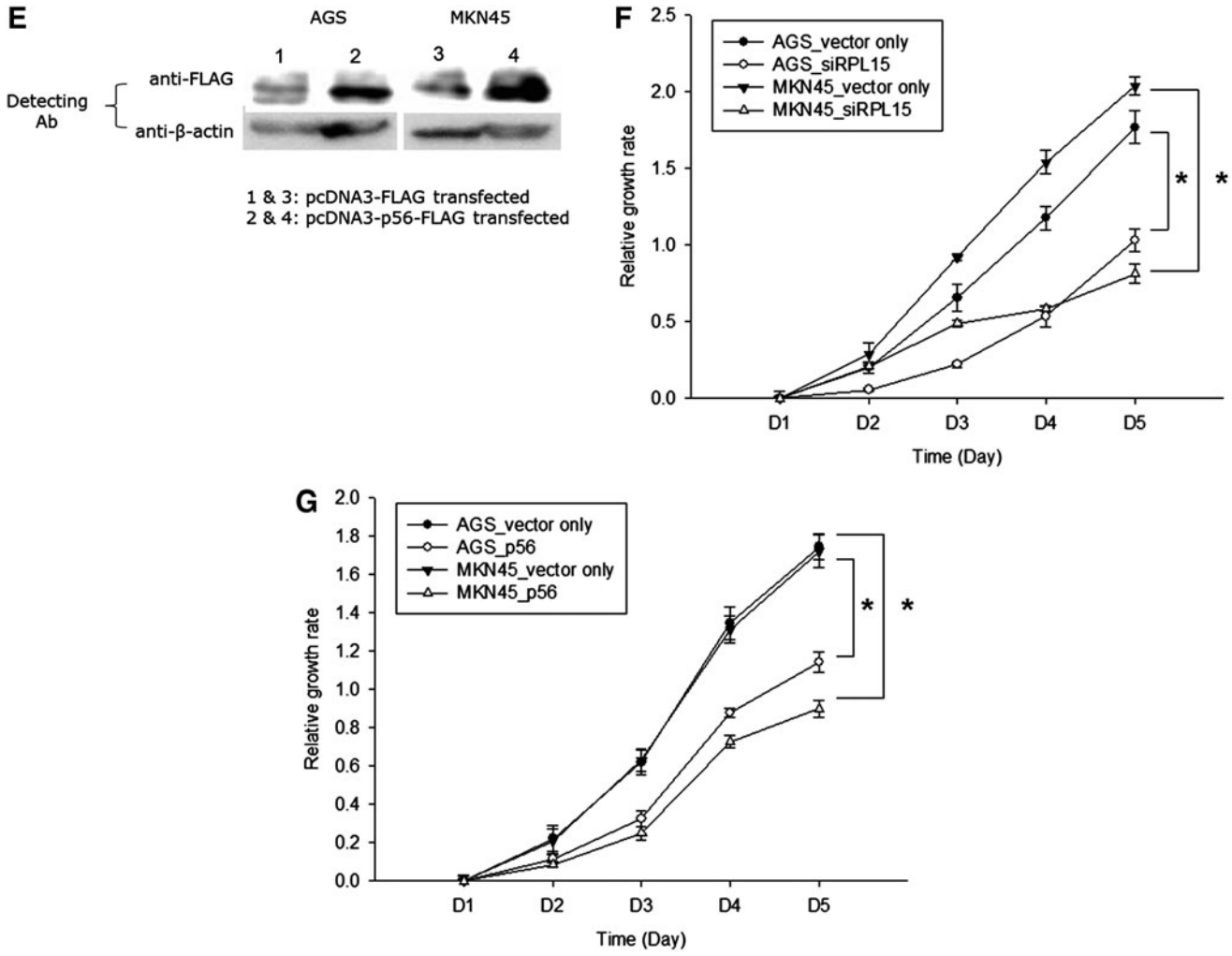


**FIG. 2.** (Continued).

bars). A similar growth inhibition phenomenon was also observed in MKN45-siRPL15 cells (Fig. 3C, black bars). On the other hand, overexpression of p56 caused a dose-dependent and significant IFN-induced antiproliferation effect on both AGS and MKN45 gastric cancer cells (Fig. 3B, D, black bars). These results indicated that either knockdown of RPL15 or overexpression of p56 contributed to the enhancement of type I IFN-induced antiproliferation effects on the gastric cancer cells.

### *TPR 1–4 domains of p56 are crucial for interacting with RPL15*

To further investigate the structural requirements of p56-RPL15 interaction, we constructed a series of FLAG-tagged p56 with truncated TPR domains (p56-TPR-FLAG), denoted as Δ1-2, Δ3-4, and Δ5-6, respectively (Fig. 4A). Plasmids carrying p56-TPR-FLAG were cotransfected with Myc-tagged RPL15 plasmid into MKN45 cells. Cell lysates from transfectants were subjected to coimmunoprecipitation using either anti-FLAG or anti-Myc agarose, and bound proteins were detected with HRP-conjugated anti-FLAG Abs by western blotting. All three p56-TPR mutants can be successfully pulled down by the anti-FLAG agarose (Fig. 4B, lane 3 in all panels), and the presence of RPL15-Myc did not affect p56 binding to the anti-FLAG agarose (Fig. 4B, lane 1 in all panels). However, when either TPR domains 1–2 or 3–4 were deleted, p56 essentially lost its binding ability with RPL15-Myc (Fig. 4B, lane 2 in top and middle panels). On the contrary, the p56-TPRΔ5-6 mutant still bound with RPL15-Myc (Fig. 4B, lane 2 in bottom panel). These results suggested that the region spanning p56 N-terminal TPR domains 1–4 is structurally important for p56-RPL15 interaction to occur.

## Discussion

We successfully identified RPL15 as a p56-interacting protein from a T7 phage display library. As a structural component of the ribosomal 60S subunit, RPL15 participates in protein synthesis and in the pathogenesis of gastric and esophageal cancers (Wang *et al.*, 2001, 2006). Suppression of the growth of SGC7901 gastric cells was observed when cells were transfected with vectors carrying siRNA for RPL15 (Wang *et al.*, 2006), a phenomenon also seen in our study (Fig. 2C). Moreover, downregulation of RPL15

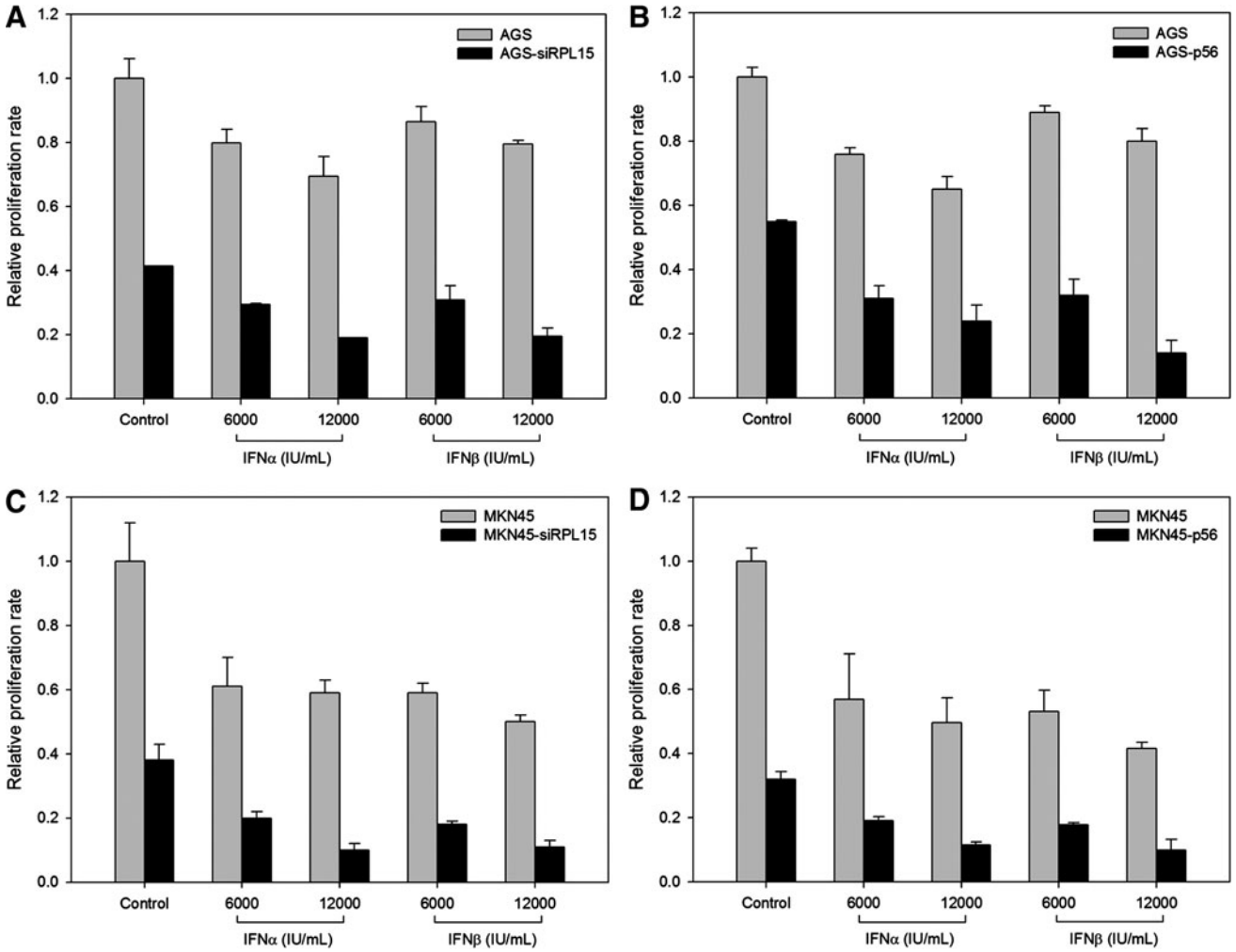


**FIG. 3.** Knock-down of RPL15 or overexpression of p56 enhanced interferon (IFN)-induced antiproliferation. AGS and MKN45 gastric cancer cells were transfected with RPL15 siRNA **(A, C)** or p56-carrying plasmid **(B, D)**, respectively. At 24 h post-transfection, two different concentrations (6000 and 12000 IU/mL) of IFNα or IFNβ were added into the cell cultures for another 48 h followed by measurement of proliferation by MTT assay. For untransfected (gray bars) and transfected (black bars) cells, the relative inhibition of proliferation was calculated by dividing the results of MTT assay of IFNα- or IFNβ-treated cells by that of the untreated control cells. All values are presented as mean ± SD for three independent experiments.

can also reduce its tumorigenicity in nude mice (Wang *et al.*, 2006). The rates of protein synthesis and expression of translation-associated proteins are significantly elevated in some tumors. These indicate that both ribosomal functions and translational control are potentially important in tumor progression.

Type I IFNs have pleiotropic effects on various target cells. For example, stimulation of apoptosis by type I IFNs is involved in Fas-associated death domain (FADD)/caspase-8 signaling, induction of the caspase cascade, release of mitochondrial cytochrome c, perturbations in mitochondrial membrane potential, changes in plasma membrane potential, alterations in plasma membrane symmetry, and DNA fragmentation (Pfeffer *et al.*, 1998; Parmar and Platanias, 2003; Pokrovskaja *et al.*, 2005). In addition to triggering apoptosis, type I IFNs can also reduce the growth rate of cancer cells; however, the underlying mechanisms are not fully understood. p56 may interact with eIF3e through its TPR 5–6 domains to inhibit protein synthesis and may contribute to the growth inhibition effect of type I IFN (Guo *et al.*; 2000). IFNα can have effects on both expression and activity of components of the protein synthesis machinery such as the eukaryotic initiation factor-5A and the eukaryotic elongation factor 1A (Caraglia *et al.*, 1997; Lamberti *et al.*, 2007). This interaction has a role in the induction of antiproliferative effects induced by IFNα (Caraglia *et al.*, 2003). Therefore, our data should be included in a more general context of connection between protein synthesis and IFN-induced signaling. In our current study, we demonstrated that either RPL15 knock-down or p56 overexpression contributed to the growth inhibition (59% and 68%, respectively) of human gastric cancer cells (Fig. 2C, D). Additionally, either RPL15 knock-down (Fig. 3A, C, black bars) or p56 overexpression (Fig. 3B, D, black bars) in both AGS and MKN45 significantly enhanced the sensitivity to IFN-induced proliferation inhibition (Fig. 3A, D, black bars). This result suggested that differential expression of RPL15 and p56 might further enhance the inhibitory

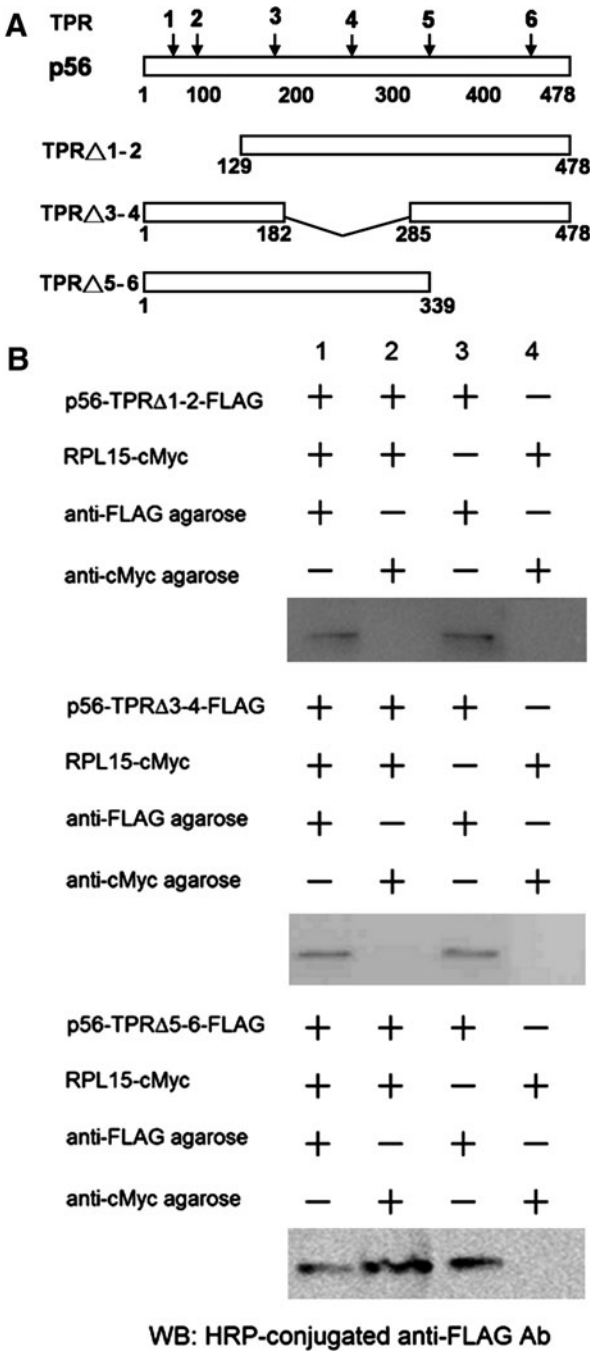


**FIG. 4.** Mapping of p56 tetratricopeptide repeat (TPR) domains crucial for interacting with RPL15. **(A)** A schematic representation of the full-length p56 and three p56 TPR deletion mutant constructs. Numbered arrows indicate the approximate locations of TPR domains in p56. The three TPR deletion mutant constructs (Δ1-2, Δ3-4, and Δ5-6) were designed so that a.a. 1–129, 183–284, and 340–478 spanning the indicated TPR domains were removed, respectively. **(B)** FLAG-tagged p56 TPR deletion mutants and cMyc-tagged RPL15 were cotransfected into MKN45 cells. At 24-h post-transfection, proteins were extracted from cell lysates and incubated with anti-FLAG-agarose, anti-cMyc-agarose, or both at 4°C for overnight with continuous stirring. The agarose-bound proteins were subsequently eluted and subjected to SDS-PAGE followed by western blotting with HRP-conjugated anti-FLAG Abs for visualization.

capacity of IFN on tumor growth, a phenomenon warranted for further investigation due to the known cytotoxicity of IFN treatments in clinical setting.

Our results also demonstrated, for the first time, that TPR 1–4 domains of p56 are crucial for the p56-RPL15 interaction to occur (Fig. 4B). TPR motifs are present in all p56 family members, which participate in the binding with other proteins. After IFN treatments of cells, high levels of p56 can be induced, whereas expression of p56 normally occurs in untreated cells. Since p56 contains six TPR motifs, it is believed that p56 interacts with several different proteins to execute its biological function. p56 may elicit cellular regulatory effects through its interaction with eIF3e or RPL15. In virus-infected cells, a similar regulatory pathway may be present, because p56 can be induced to high levels by double-stranded RNA in an IFN-independent manner.

In summary, we had found a new possible mechanism of resistance to type I IFNs in cancer cells. Our current results demonstrated that p56 interacts with RPL15, with the TPR domains 1–4 of p56 being structurally indispensable for the interaction to occur. Overexpression of p56 or down-regulation of RPL15 not only contributed to the growth inhibition on gastric cancer cells but also increased the sensitivity of IFN-induced proliferative inhibition. PRL15, as a crucial 60S ribosomal subunit component, participates in protein synthesis and contributes to the antiproliferative effects of type I IFN. The antiproliferative effect of type I IFN is mediated through various possible mechanisms such as by interacting with eukaryotic initiation factor 3e (eIF3e) subunit of eIF3 complex to inhibit protein synthesis and, thus, inhibit growth of the cells. p56 contains six different TPR motifs, a domain known for protein-protein interaction. With six different TPR, motifs tend to bind to various proteins and exert various biological functions. In the present study, we have found that overexpression of p56 in RPL15 overexpressed gastric cancer cells can inhibit the growth of the cells, and inhibiting the RPL15 expression level by siRNA shows the same effect on those cells. p56 and RPL15 are interacting partners. Taken together, although indirectly, we conclude that the antiproliferative effect of p56 is likely mediated through its interacting with RPL15. Therefore, further investigation into the detailed mechanisms by which p56 and RPL15 interact is warranted for the future development of pharmaceutical applications for antivirus or anticancer treatments.

## Acknowledgments

This study was supported in part by grants from the National Science Council (96-2628-B-039-002-MY3), Taipei, Taiwan, and China Medical University Hospital (DMR-97-001, DMR-97-002, and DMR-97-124), Taichung, Taiwan.

## Disclosure Statement

The authors declare no conflict of interest.

## References

Blatch, G.L., and Lassle, M. (1999). The tetratricopeptide repeat: a structural motif mediating protein-protein interactions. Bioessays **21,** 932–939.

Caraglia, M., Marra, M., Giuberti, G., D'Alessandro, A.M., Baldi, A., Tassone, P., Venuta, S., Tagliaferri, P., and Abbruzzese, A.

(2003). The eukaryotic initiation factor 5A is involved in the regulation of proliferation and apoptosis induced by interferon-alpha and EGF in human cancer cells. J Biochem **133,** 757–765.

Caraglia, M., Marra, M., Pelaia, G., Maselli, R., Caputi, M., Marsico, S.A., and Abbruzzese, A. (2005). Alpha-interferon and its effects on signal transduction pathways. J Cell Physiol **202,** 323–335.

Caraglia, M., Marra, M., Tagliaferri, P., Lamberts, S.W., Zappavigna, S., Misso, G., Cavagnini, F., Facchini, G., Abbruzzese, A., Hofland, L.J., and Vitale, G. (2009). Emerging strategies to strengthen the anti-tumour activity of type I interferons: overcoming survival pathways. Curr Cancer Drug Targets **9,** 690–704.

Caraglia, M., Passeggio, A., Beninati, S., Leardi, A., Nicolini, L., Improta, S., Pinto, A., Bianco, A.R., Tagliaferri, P., and Abbruzzese, A. (1997). Interferon alpha2 recombinant and epidermal growth factor modulate proliferation and hypusine synthesis in human epidermoid cancer KB cells. Biochem J **324 (Pt 3),** 737–741.

Goebl, M., and Yanagida, M. (1991). The TPR snap helix: a novel protein repeat motif from mitosis to transcription. Trends Biochem Sci **16,** 173–177.

Guo, J., Peters, K.L., and Sen, G.C. (2000). Induction of the human protein P56 by interferon, double-stranded RNA, or virus infection. Virology **267,** 209–219.

Guo, J., and Sen, G.C. (2000). Characterization of the interaction between the interferon-induced protein P56 and the Int6 protein encoded by a locus of insertion of the mouse mammary tumor virus. J Virol **74,** 1892–1899.

Hui, D.J., Bhasker, C.R., Merrick, W.C., and Sen, G.C. (2003). Viral stress-inducible protein p56 inhibits translation by blocking the interaction of eIF3 with the ternary complex eIF2.GTP.Met-tRNAi. J Biol Chem **278,** 39477–39482.

Hui, D.J., Terenzi, F., Merrick, W.C., and Sen, G.C. (2005). Mouse p56 blocks a distinct function of eukaryotic initiation factor 3 in translation initiation. J Biol Chem **280,** 3433–3440.

Lamberti, A., Longo, O., Marra, M., Tagliaferri, P., Bismuto, E., Fiengo, A., Viscomi, C., Budillon, A., Rapp, U.R., Wang, E., Venuta, S., Abbruzzese, A., Arcari, P., and Caraglia, M. (2007). C-Raf antagonizes apoptosis induced by IFN-alpha in human lung cancer cells by phosphorylation and increase of the intracellular content of elongation factor 1A. Cell Death Differ **14,** 952–962.

Parmar, S., and Platanias, L.C. (2003). Interferons: mechanisms of action and clinical applications. Curr Opin Oncol **15,** 431–439.

Pfeffer, L.M., Dinarello, C.A., Herberman, R.B., Williams, B.R., Borden, E.C., Bordens, R., Walter, M.R., Nagabhushan, T.L., Trotta, P.P., and Pestka, S. (1998). Biological properties of recombinant alpha-interferons: 40th anniversary of the discovery of interferons. Cancer Res **58,** 2489–2499.

Sadler, A.J., and Williams, B.R. (2008). Interferon-inducible antiviral effectors. Nat Rev Immunol **8,** 559–568.

Sarkar, S.N., and Sen, G.C. (2004). Novel functions of proteins encoded by viral stress-inducible genes. Pharmacol Ther **103,** 245–259.

Sikorski, R.S., Boguski, M.S., Goebl, M., and Hieter, P. (1990). A repeating amino acid motif in CDC23 defines a family of proteins and a new relationship among genes required for mitosis and RNA synthesis. Cell **60,** 307–317.

Terenzi, F., Hui, D.J., Merrick, W.C., and Sen, G.C. (2006). Distinct induction patterns and functions of two closely related interferon-inducible human genes, ISG54 and ISG56. J Biol Chem **281,** 34064–34071.

Terenzi, F., Pal, S., and Sen, G.C. (2005). Induction and mode of action of the viral stress-inducible murine proteins, P56 and P54. Virology **340,** 116–124.

Terenzi, F., Saikia, P., and Sen, G.C. (2008). Interferon-inducible protein, P56, inhibits HPV DNA replication by binding to the viral protein E1. EMBO J **27,** 3311–3321.

Wan, L., Kung, Y.J., Lin, Y.J., Liao, C.C., Sheu, J.J., Tsai, Y., Lai, H.C., Peng, C.Y., and Tsai, F.J. (2009). Th1 and Th2 cytokines are elevated in HCV-infected SVR(-) patients treated with interferon-alpha. Biochem Biophys Res Commun **379,** 855–860.

Address correspondence to:
*Lei Wan, Ph.D.*
*School of Chinese Medicine*
*China Medical University*
*No. 2 Yuh-Der Road*
*Taichung 40402*
*Taiwan*

*E-mail:* leiwan@mail.cmu.edu.tw

*Bing-Hung Chen, Ph.D.*
*Department of Biotechnology*
*Kaohsiung Medical University*
*100 Shih-Chuan 1st Road*
*Kaohsiung 807*
*Taiwan*

*E-mail:* bhchen@kmu.edu.tw

Received for publication September 27, 2010; received in revised form February 23, 2011; accepted February 24, 2011.